Published in final edited form as:
NMR Biomed. 2012 February ; 25(2): 332–339. doi:10.1002/nbm.1754.

Localized ^{1}H NMR Spectroscopy in Different Regions of Human Brain *In Vivo* at 7 T: T_2 Relaxation Times and Concentrations of Cerebral Metabolites

Małgorzata Marjańska[a], **Edward J. Auerbach**[a], **Romain Valabrégue**[b], **Pierre-François Van de Moortele**[a], **Gregor Adriany**[a], and **Michael Garwood**[a]

[a]Center for Magnetic Resonance Research and Department of Radiology, University of Minnesota, 2021 6thST SE, Minneapolis, Minnesota 55455, United States

[b]CRICM (CENIR), UPMC/INSERM UMRS 975/CNRS UMR 7225, Hôpital Pitiè-Salpêtriére, Paris, France

Abstract

At the high field strength of 7 T, *in vivo* spectra of the human brain with exceptional spectral quality sufficient to quantify sixteen metabolites have previously been obtained only in the occipital lobe. However, neurochemical abnormalities associated with many brain disorders are expected to occur in brain structures other than the occipital lobe. The purpose of the present study was to obtain high quality spectra from various brain regions at 7 T and to quantify the concentrations of different metabolites. To obtain concentrations of metabolites within four different regions of the brain such as occipital lobe, motor cortex, basal ganglia, and cerebellum, the T_2 relaxation times of the singlets and *J*-coupled metabolites in these regions were measured for the first time at 7 T. Our results demonstrate that high quality, quantifiable spectra can be obtained in regions other than the occipital lobe at 7 T utilizing a 16-channel transceiver coil and B_1^+ shimming.

Keywords

occipital lobe; motor cortex; basal ganglia; cerebellum; LCModel

Introduction

Proton Magnetic Resonance Spectroscopy (^{1}H MRS) provides a noninvasive way to investigate *in vivo* neurochemical abnormalities of many brain disorders. Each observable metabolite can potentially provide unique information about brain biochemistry and be a biomarker for brain disorders to facilitate diagnosis and treatment. MRS data can be obtained using either chemical shift imaging (CSI) or single-voxel localization. In general, CSI data are usually acquired within a slice and allow the quantification of a limited number of metabolites (up to eight) (1–4). Three-dimensional (3D) CSI acquisitions at 3 T enabled the detection of five metabolites (5). Previous 3D CSI acquisitions performed at 7 T had a limited spatial coverage and five metabolites were detected without the ability to distinguish between glutamate and glutamine (6, 7). On the other hand, single-voxel data can be potentially obtained from any brain region, and up to sixteen metabolites can be quantified (8, 9). At the high field strength of 7 T, exceptional spectral quality that allows for the

Corresponding author: Małgorzata Marjańska, Ph.D., Center for Magnetic Resonance Research, 2021 6th Street SE, Minneapolis, MN 55455, United States, Phone: 1-612-626-2001, Fax: 1-612-626-2004, gosia@cmrr.umn.edu.

quantification of sixteen metabolites has been previously obtained in occipital lobe (8–12). However, neurochemical abnormalities for many brain disorders are expected to occur in brain regions other than the occipital lobe.

Previous single-voxel 7 T studies that measured sixteen different neurochemicals used localization techniques with short echo time (6 ms in STEAM (8) and SPECIAL (9)). The absolute quantification when using these techniques is straightforward since there is no need to consider *J* evolution and T_2 relaxation. An alternative single-voxel technique is a fully-adiabatic spin-echo localization by adiabatic selective refocusing (LASER) (13) sequence, which is a single-shot sequence that generates very sharp localization edges without the need for outer-volume suppression. The adiabatic full passage (AFP) pulses used in LASER are robust to radio frequency (RF) field changes, which makes them very advantageous at high fields where B_1 inhomogeneity is problematic. The available peak RF power also does not limit the bandwidth which minimizes the voxel displacement. However, LASER tends to require a relatively long echo time. To shorten the echo time, the adiabatic half passage (AHP) pulse and one pair of AFP pulses can be replaced with a single slice selective pulse (14, 15). Even with that replacement, the echo time is much longer than 6 ms used in the STEAM or SPECIAL sequences. To obtain absolute concentrations of metabolites from spectra obtained at longer echo times, the knowledge of both the *J*-modulation and T_2 relaxation times is required. The T_2 relaxation times at 7 T have been reported previously for the methyl protons of *N*-acetylaspartate (NAA) and the methyl protons of total creatine (creatine + phosphocreatine, tCr) (10, 16).

The measurement of T_2 for *J*-coupled metabolites is more difficult as their signal intensity is decreased with echo time and their spectral pattern changes due to *J*-evolution. For reliable T_2 measurements, the signal changes due to *J*-modulation need to be taken into account by simulating the spectral pattern at each time. Additional complications arise from the overlap of resonances from different molecules and macromolecule contributions. Recently, T_2 relaxation times of *J*-coupled cerebral metabolites in rat at 9.4 T were obtained using simulated echo time (T_E) specific basis sets and LCModel analysis (17). Excellent fits were obtained when each metabolite was considered as one component except for NAA and tCr which were split into NAA methyl and aspartate moieties, and CH_3 and CH_2 groups, respectively suggesting that correct prior knowledge was used to perform the analysis.

The aim of the present study was to investigate the efficacy of using the LASER sequence to obtain high quality 7 T spectra from brain regions other than occipital lobe, to measure T_2 relaxation times in different brain regions of the singlets and *J*-coupled metabolites, and to quantify concentrations of metabolites in different brain regions. The obtained results show that high quality, quantifiable spectra can be obtained *in vivo* at 7 T in regions of the brain other than the occipital lobe.

Experimental

Subjects

Healthy, normal volunteers ($n = 23$, 12 M, 11 F, age: 23 ± 4 years) were studied after giving informed consent according to the procedures approved by the Institutional Review Board of the University of Minnesota Medical School.

MR Acquisition

In vivo data were obtained on a 7-T, 90-cm horizontal bore magnet (Magnex Scientific Inc., Oxford, UK) interfaced with a Siemens TIM console (Siemens, Erlangen, Germany). The magnet was equipped with a gradient coil capable of reaching 40 mT/m in 200μs. A 16-channel transmission line head array RF coil (18) was used to transmit and receive. The

transmit phase of each coil channel was controlled with independent 1 kW RF amplifiers (CPC, Brentwood, NY, USA). A RF power monitoring system measured forward and reflected power for each channel to ensure that local specific absorption rate remained below 3 W/kg.

Turbo spin echo (TSE) images (repetition time, T_R = 3 s, echo time, T_E = 95 ms, field-of-view, FOV = 26 × 26 cm^2, matrix = 256 × 256, slice thickness = 1.5 mm, 66 slices, acquisition time = 4 min) were acquired with a 22.5° RF transmit phase difference between adjacent elements (standard transmit phases) to select the volumes of interest (VOI) in occipital lobe (OC, 2.7 × 2.7 × 2.7 cm^3), motor cortex (MC, 2 × 2 × 2 cm^3), basal ganglia (BG, 1.5 × 4 × 1.5 cm^3), and cerebellum (CR, 2.5 × 2.5 × 2.5 cm^3). The occipital VOI was positioned symmetrically within the occipital lobes of both hemispheres. The motor cortex VOI was centered on the hand knob, which corresponds to the primary motor cortex of the upper limb representation (19). The basal ganglia VOI was positioned in the lentiform nucleus and therefore included the putamen and globus pallidus. The cerebellar VOI was placed symmetrically about the midline and mainly included the cerebellar vermis.

Low flip angle gradient echo images were acquired for B_1^+ shimming by pulsing RF power through one channel at a time and receiving the signal with all 16 channels (T_R = 60 ms, T_E = 3.6 ms, FOV = 168 × 256 cm^2, nominal flip angle = 15°, slice thickness = 4 mm, total acquisition time = 2.5 min). For each voxel, the B_1^+ phase was optimized based on a previously published algorithm (20). A set of transmit phases determined by B_1^+ shimming improved transmit efficiency by a factor of 2 ± 0.5 (mean and standard deviation) in the occipital lobe, 1.31 ± 0.09 in the motor cortex, 1.35 ± 0.04 in the basal ganglia, and 3 ± 1 in the cerebellum when compared to standard transmit phases.

All spectra were acquired using a LASER sequence in which the AHP pulse and two AFP pulses were replaced with a slice-selective 90° Hamming-filtered sinc pulse (14, 15), a pulse length of 1.52 ms and a bandwidth of 5.84 kHz. The two other dimensions were selected with a pair of hyperbolic secant pulses, HS1 (13, 21, 22), with a pulse length T_p of 5.12 ms and a bandwidth of 3.92 kHz. Each voxel measurement began with a calibration of the localized B_1^+ field strength and an adjustment of the first- and second-order shims using FAST(EST)MAP (23, 24). The water suppression module consisted of variable power and optimized relaxation delays (VAPOR) and outer volume suppression (OVS) (25) in the direction of slice excitation only. These modules were adapted for the human 7 T system and incorporated prior to the excitation pulse in LASER. The repetition time was 4.5 s.

Each free induction decay (FID) was acquired with 2048 complex points using a spectral width of 4 kHz. FIDs were stored separately in memory and then frequency and phase corrected based on either the NAA signal at 2.01 ppm or the tCr signal at 3.03 ppm prior to summation.

For the T_2 measurement, the echo time was extended by adding delays around the last AFP pulse in the sequence, and the spectra were collected at six echo times: 35, 70, 105, 140, 175, 210 ms. For all echo times, 64 averages were acquired. Macromolecular (MM) spectra were acquired using the inversion recovery technique (26) (T_R = 2 s, T_{IR} = 900 ms, number of scans (N_S) = 1920 (T_E = 35 ms), N_S = 1664 (T_E = 70), N_S = 1664 (T_E = 105 ms), and N_S = 512 (T_E = 140 ms)) in the occipital lobe of five subjects for all T_E's except 175 and 210 ms where the MM signal was very weak. For assessing regional differences in metabolite concentrations, spectra were acquired with an echo time of 35 ms and 128 averages.

Spectral Fitting

The acquired spectra were analyzed using LCModel 6.1-4A (27, 28) (Stephen Provencher, Inc., Oakville, Ontario, Canada), which calculates the best fit of the experimental spectrum as a linear combination of model spectra. The basis set for LCModel was generated using home-written programs based on the density matrix formalism (29) in Matlab (The MathWorks, Inc., Natick, MA, USA) using the known chemical shifts and *J*-couplings (30, 31). In addition, a small signal was added at 0 ppm in all basis spectra for automatic frequency referencing. The simulated spectra of the following twenty one metabolites were included in the basis set for LCModel: alanine (Ala), ascorbate (Asc), aspartate (Asp), creatine (Cr), γ-aminobutyric acid (GABA), glucose (Glc), glutamine (Gln), glutamate (Glu), glycerophosphorylcholine (GPC), glycine (Gly), glutathione (GSH), lactate (Lac), *myo*-inositol (*m*Ins), NAA, *N*-acetylaspartylglutamate (NAAG), phosphocreatine (PCr), phosphorylcholine (PCho), phosphorylethanolamine (PE), *scyllo*-inositol (*s*Ins), taurine (Tau) and threonine (Thr). Three metabolites, NAA, Cr, and PCr, were separated into different moieties, and independent spectra for the singlet (CH_3 group, sNAA) and the multiplet (CH_2 group, mNAA) of NAA and the singlet of the CH_3 and CH_2 groups of tCr were included in the basis set. No baseline correction, zero-filling or line broadening were applied to the *in vivo* data prior to the analysis.

The experiment MM spectrum (average from five subjects) from occipital region at each T_E was included in the basis set, except for T_E of 175 and 210 ms. The methylene protons peak of tCr at 3.93 ppm was present in the MM spectra due to a shorter T_1 relaxation time (26) and was removed in the time domain using the HSVD Lanczos algorithm from MRUI 99.2b (32). The LCModel fitting was performed over the spectral range from 0.5 to 4.2 ppm.

Signal to Noise Ratio Calculation

Signal to noise ratios (SNR) for various metabolites were calculated using prior knowledge and taking the ratio of the maximum signal for the particular metabolite minus baseline over root mean square of the noise measured between 0.2 and 0.4 ppm. No line-broadening was applied.

T_2 fitting

The T_2 values of various metabolites were determined by fitting the concentrations obtained from an LCModel analysis (without water scaling) using a two parameter mono-exponential decay function with a non-linear least square algorithm (nlinfit) in Matlab. The goodness of fit was evaluated using corrcoef function in Matlab which returns p values for testing the hypothesis of no correlation. If the p value is small, then the correlation is significant.

Quantification

Quantification was obtained using the unsuppressed water signal obtained from the same voxel (33). Concentrations were corrected for cerebrospinal fluid (CSF) content. The tissue composition was measured using TSE images, which were segmented into gray matter (GM), white matter (WM) and CSF content using the segmentation function of SPM8 software (www.fil.ion.ucl.ac.uk/spm). The fractional volumes of GM, WM and CSF were obtained by averaging the gray/white and CSF segmented images over the spectroscopic voxel. The relative densities of MR-visible water for GM, WM, and CSF were assumed to be 0.78, 0.65, 0.97 (34), respectively. The T_1 and T_2 relaxation times of water used in the calculation of the attenuation factors were taken from published reports (T_1(GM) = 2130 ms, T_1(WM)= 1220 ms, T_1(CSF) = 4425 ms (35); T_2(GM) = 50 ms, T_2(WM) = 55 ms, T_2(CSF) = 141 ms (36)). The water attenuation was computed using the fractional volume of each compartment. For the basal ganglia voxel, the values of 1523 ms for T_1 and 41.2 ms for T_2

of water were used based on the previously reported T_1 values of water in putamen and globus pallidus (35) and T_2 measured in this study (Table 1), respectively. For the cerebellum, the value of 48 ms was used for T_2 of water (Table 1). The T_1 relaxation for the metabolites was not taken into consideration as an attenuation factor since this would be very small due to the use of repetition time of 4.5 s. The T_2 of the metabolites obtained in this study were used. The T_2's of the metabolites which we were unable to measure were assumed to be similar to that of *m*Ins (37), while Gln and NAAG were considered to have similar T_2 values as Glu and the singlet of NAA, respectively.

The criteria for selecting reliable metabolite concentrations were based on the Cramér-Rao lower bounds (CRLB), which are estimates of the %SD of the fit for each metabolite (27). Only results with a CRLB ≤50% were included in the analysis. Concentrations with CRLB > 50% were classified as not detected. If the covariance between two metabolites was consistently high (correlation coefficient < −0.5), such as was found for Cr and PCr, their sum was reported.

Statistical Analysis

Statistical analysis was conducted using SAS Software for Windows (version 9.1, SAS Institute, Cary, NC). One-way analysis of variance (ANOVA) with a Tukey post hoc test was used to compare the T_2 relaxation times and the concentrations at each location for each metabolite. This is appropriate because a different set of subjects was used to estimate concentrations and relaxation times and thus the four regions represent four independent groups. A two-sample paired t-test was used to compare the T_2 relaxation times between sNAA and mNAA, and between tCr at 3.03 ppm and 3.93 ppm. The paired t-test was used to account for the correlation between two moieties of the same metabolite from the same subject.

Results and Discussion

Spectral Quality

In Figure 1, boxes drawn on the T_2-weighted images of a human brain obtained at 7 T show the position and size of the localized volumes from where the spectra were acquired. Voxels of different sizes were placed over the occipital lobes in both hemispheres, the primary motor cortex of the upper limb representation, the basal ganglia in lentiform nucleus and the cerebellum. The spectra shown in Figure 1 are representative of the quality consistently obtained using a modified LASER sequence in this study.

The spectra were of very high quality without any contamination from signals outside the voxel such as the lipid signal which suggested that the modified LASER sequence was very efficient in suppressing signals from outside of the voxels. Similar linewidths of water (13 ± 1 Hz in OC, 11 ± 2 Hz in MC, 14 ± 1 Hz in CR, and 21 ± 4 Hz in BG) and tCr (12 ± 2 Hz in OC, 12 ± 1 Hz in MC, 11 ± 1 Hz in CR, and 22 ± 2 Hz in BG) were obtained in all regions except for the basal ganglia. The linewidths of water and total creatine were very similar to each other in all voxels. In the basal ganglia, it turned out to be more difficult than in other regions to achieve good field homogeneity by localized shimming, possibly due to the heterogeneity of the tissue included in the voxel. The variation of the signal-to-noise ratio in these four spectra is mainly due to the differences in the voxel size and linewidths. Additionally, the residual of the basal ganglia spectrum has uneven noise due to poorly spoiled water signal. The spectral quality was degraded in the basal ganglia region due to a 10 Hz linewidth difference between the spectra obtained in the basal ganglia and other regions. Excellent water suppression was also consistently achieved, as illustrated by the small water residual observed in all subjects (data not shown) and by the flat baseline (Figure 1).

It was possible to obtain these spectra due to our ability to control the amount of available B_1^+ over a particular region of interest using local B_1^+ shimming (20). Figure 2 demonstrates the gain in transmit B_1 obtained after local B_1^+ shimming. With the standard phase arrangement, the most efficient transmission was at the center of the brain, but even for the two voxels located relatively close to the center of the brain, motor cortex and basal ganglia, the gain in the transmit efficiency was significant (~1.3). The biggest gain in transmit efficiency was observed for the voxels located in the periphery such as in the cerebellum and occipital lobe.

T_2 Relaxation Times

Figure 3 shows the quality of representative spectra obtained from the occipital lobe at different echo times from one volunteer. The singlet resonances become smaller with increasing echo time while the multiplet resonances undergo *J* modulation. The macromolecule resonances (especially visible between 0.5 and 1.9 ppm) also undergo *J* evolution, which can be clearly seen from the inversion of the macromolecular resonances in the spectrum acquired at an echo time of 105 ms. Due to their short T_2 and scalar coupling, macromolecular resonances decrease as a function of echo time, and after 140 ms, these signals are below the thermal noise level. As a result, long echo time spectra are characterized by a flat baseline in the region between 0.5 and 1.9 ppm. In acquiring the macromolecular spectra, the decreased relative contribution of macromolecular signals to the overall spectrum allowed the number of averages to be reduced as the echo time increased without having an affect on the quality of the fits.

The SNR for tCr at 3.03 ppm as a reference and *J*-coupled metabolites are reported in Table 2 for the data displayed in Figure 3. The SNR for *J*-coupled metabolites reflects the effect of both T_2 relaxation and *J* evolution. The lowest SNR values of 1.95 for GSH and 3.8 for Tau demonstrate that these metabolites can be readily detected at all echo times.

The mean values and standard deviations (SDs) for the T_2 values of water and metabolites measured at 7 T in four brain regions are listed in Table 1. The mean R^2 values, which indicate the accuracy of the exponential fits, are also listed in Table 1. The relative SDs were typically 5% to 10%, but were larger for the aspartyl resonances of NAA (mNAA) in all the brain regions, for all metabolites in the basal ganglia, for *s*Ins, Tau and GSH resonances in the cerebellum, and for the *m*Ins and Tau resonances in the motor cortex. Additionally, the goodness of fit was evaluated and p values are reported in Table 1. All *p* values were below 0.04 except for mNAA in cerebellum and GSH in motor cortex which suggested that good quality fits were obtained for all metabolites in all regions except for those four cases.

The T_2 relaxation times of water were the same in all voxels except for the basal ganglia where it was significantly shorter. The T_2 value obtained for water in the relatively large occipital lobe voxel containing GM, WM, and CSF was within the standard deviation of the T_2 previously measured in the GM and slightly shorter than average value plus the standard deviation of the T_2 previously measured in the WM with LASER at 7 T (36).

The T_2 values for sNAA ranged from 130 to 191 ms in different brain regions. In the occipital lobe and the basal ganglia, T_2's of sNAA were the same and were significantly shorter than in the motor cortex and the cerebellum. In this study, the T_2 value obtained in the occipital lobe was in agreement with the lower end of the published T_2 range (10, 16).

The T_2 values for the methyl protons of tCr ranged from 90 to 131 ms in different brain regions. They were the same in the occipital lobe and the basal ganglia, but significantly longer in the cerebellum. In the motor cortex, the T_2 value for the tCr peak at 3.03 ppm was not significantly different from that found in the cerebellum and the occipital lobe, but it was

significantly longer than that found in the basal ganglia. The measured T_2 relaxation time for tCr (CH_3 peak) in the occipital lobe, 95 ± 3 ms, was within a standard deviation of previously measured values at 7 T (10, 16).

Other relaxation times reported in Table 1 for both singlets and *J*-coupled metabolites were measured for the first time at 7 T in human brain. The T_2 value for mNAA was significantly shorter in the occipital lobe region ($p = 0.006$) than for sNAA while there was no significant difference between the T_2 values of sNAA and mNAA in the basal ganglia and the cerebellum. In the motor cortex, a tendency for the T_2 of mNAA to be shorter (p = 0.096) than the T_2 of sNAA was observed. It has been previously reported that there is a significant difference between T_2 relaxation times of sNAA and mNAA in the parieto-occipital lobe (38). In that study and this study, the signal of mNAA decayed faster than the sNAA signal. Additionally, a significant difference in the relaxation times for sNAA and mNAA has been reported in rat brain at 9.4 T (17).

The T_2 values for the tCr peak at 3.93 ppm ranged from 81 to 108 ms and were significantly shorter than that found for the 3.03 ppm singlet in the occipital lobe ($p = 0.0023$) and in the cerebellum ($p = 0.0164$). The observed difference between the relaxation times of the tCr peaks at 3.03 ppm and 3.93 ppm has been reported previously (39). Additionally, the T_2 of tCr (CH_2 peak) was significantly longer in the motor cortex than in the occipital lobe and basal ganglia.

The T_2 for the other singlets, tCho and *s*Ins, ranged in values from 121 to 200 ms and 80 to 130 ms, respectively. The longest T_2 value for tCho was obtained in the cerebellum, and the shortest was found in the basal ganglia. The T_2 values for *s*Ins and the methyl protons of tCr were very similar in all brain regions.

The T_2 values obtained for the *J*-coupled metabolites measured in this study were generally shorter than the T_2 values found for the singlets. In the occipital lobe, the T_2's of the *J*-coupled metabolites were very similar to the T_2 of the methyl protons of tCr except for the T_2 of GSH which was shorter. The longest T_2's of the *J*-coupled metabolites were measured in the cerebellum. The T_2 of the *J*-coupled metabolites was not significantly different in the occipital lobe, motor cortex and basal ganglia voxels. Due to the difference in the quality of the spectra, it was not possible to obtain the T_2 of GSH in the basal ganglia.

Quantification of Spectra at T_E = 35 ms

The concentrations of metabolites (means and standard deviations) obtained from four brain locations after fitting spectra using the LCModel and correcting for T_2 relaxation of water and metabolites, water tissue content, and CSF contribution, are listed in Table 3. Additionally, CRLBs are reported in Table 3 to reflect the estimated errors in quantification. The quality of the LCModel fits is shown in Figure 1 for each brain region. The baselines were flat with very small oscillations which most probably were due to differences arising from macromolecular spectrum, and the residuals were small without any noticeable resonances. The residual in the basal ganglia voxel was noisier than for other voxels due to the small size of the voxel and the broader linewidths than in other brain locations.

Sixteen metabolites were quantified with the CRLBs below 30% in the occipital lobe, motor cortex, and cerebellum, and fifteen in basal ganglia, where it was not possible to quantify glycine. The CRLBs for the dominant metabolites (e.g. NAA, tCr, tCho, mIns, Glu) were found to be below 5% in all brain regions and were comparable to those obtained previously at 7 T in occipital lobe using either STEAM (11, 12) or SPECIAL (9). The CRLBs for other metabolites were below 30% and were comparable to those obtained previously in the occipital lobe (9, 11, 12) except for Gln, NAAG, and Asc which were higher in this study.

The concentrations of metabolites obtained in the occipital lobe agreed well with previously published 7 T studies (9, 11, 12). The concentrations of two metabolites namely Gln and NAAG were lower in this study than in previously published work (9, 11, 12). For these metabolites, the T_2 relaxation times were unknown in human brain at 7 T and were assumed to be similar to either Glu (in the case of Gln) or sNAA (in the case of NAAG).

Regional differences in the concentrations of the different metabolites were detected. The highest levels of tCr, tCho, Glc + Tau, Gln and *m*Ins were detected in the cerebellum which agrees with previously published data (40, 41). The lowest level of Glu was detected in the motor cortex and the basal ganglia, while the highest level of GABA was detected in the basal ganglia. Metabolites such as GSH, sIns, and Lac + Thr were found to be uniformly distributed in all voxels.

Quantification of metabolites can be affected by T_1 and T_2 values of both water and metabolites. In the basal ganglia voxel, tissue heterogeneity is expected to lead to a range of water T_1 values. Despite this, the effect of the uncertainty in T_1 of water in the basal ganglia voxel on the measured concentration of metabolites was estimated to be only 2%. In the occipital cortex, lower than expected concentration of Gln was observed, which can be potentially caused by the fact that the same T_2 relaxation time was used for both Glu and Gln since we were not able to measure the T_2 of Gln in this study. Perhaps, there is a significant difference between T_2 of those two molecules in the occipital cortex.

Metabolite quantification when using moderate to long echo time techniques necessitates measurement of relaxation times which has the disadvantage of increasing scan time, unless the relaxation times are known *a priori* and are known not to change with disease. In addition, in our approach the relaxation times of different moieties in the same molecule are assumed to be the same (e.g., Glu). However, T_2 of metabolites has been shown to change in schizophrenia (42).

Conclusions

In this study, excellent quality spectra were obtained at 7 T using modified LASER sequence that enabled the quantification of fifteen metabolites in four regions of human brain. The quantification was performed taking into consideration CSF content, tissue composition, the relative density of MR-visible water, the T_1 and T_2 relaxation times of water in different tissue types, and the T_2 relaxation of metabolites measured in this study. The observed concentrations in the occipital lobe agreed with previously reported values obtained using short echo time techniques. Regional differences in the T_2 relaxation times as well as concentrations were detected and agreed with previous reports. The obtained results demonstrate that similar quality spectra can be obtained at 7 T in brain regions other than the occipital lobe and that quantification of longer echo time spectra is possible.

Acknowledgments

The authors thank Joanna Lukas and Stephen D. Weigand for help with statistics, Dinesh Deelchand, Pierre-Gilles Henry, Stéphane Lehéricy and Patrick Bolan for helpful discussion, and Jamie D. Walls for comments about the paper.

Sponsors: This work was supported by NIH: BTRC P41 RR008079, P30 NS057091, and the W.M. Keck Foundation.

List of abbreviations

AFP adiabatic full passage

AHP	adiabatic half passage
Ala	alanine
ANOVA	analysis of variance
Asc	ascorbate
BG	basal ganglia
CR	cerebellum
Cr	creatine
CRLB	Cramér-Rao lower bounds
CSF	cerebrospinal fluid
FID	free induction decay
GABA	γ-aminobutyric acid
Glc	glucose
Gln	glutamine
Glu	glutamate
Gly	glycine
GM	gray matter
GPC	glycerophosphorylcholine
GSH	glutathione
Lac	lactate
LASER	localization by adiabatic selective refocusing
MC	motor cortex
***m*Ins**	*myo*-inositol
MM	macromolecules
mNAA	aspartyl resonances of NAA, NAA multiplet
NAA	*N*-acetylaspartate
NAAG	*N*-acetylaspartylglutamate
N_S	number of scans
OC	occipital lobe
OVS	outer volume suppression
PCho	phosphorylcholine
PCr	phosphocreatine
PE	phosphorylethanolamine
RF	radio frequency
SD	standard deviation
***s*Ins**	*scyllo*-inositol
sNAA	methyl resonance of NAA, NAA singlet

SPECIAL	spin-echo, full intensity acquired localized
STEAM	stimulated echo acquisition mode
Tau	taurine
tCho	total choline, GPC + PCho
tCr	total creatine, creatine + phosphocreatine
T_E	echo time
Thr	threonine
T_{IR}	inversion time
T_R	repetition time
TSE	turbo spin echo
VAPOR	variable pulse power and optimized relaxation delays
VOI	volume of interest
WM	white matter

References

1. Pan JW, Twieg DB, Hetherington HP. Quantitative spectroscopic imaging of the human brain. Magn Reson Med. 1998; 40(3):363–369. [PubMed: 9727938]
2. Posse S, Otazo R, Caprihan A, Bustillo J, Chen HJ, Henry PG, Marjanska M, Gasparovic C, Zuo C, Magnotta V, Mueller B, Mullins P, Renshaw P, Ugurbil K, Lim KO, Alger JR. Proton echo-planar spectroscopic imaging of *J*-coupled resonances in human brain at 3 and 4 Tesla. Magn Reson Med. 2007; 58(2):236–244. [PubMed: 17610279]
3. Balchandani P, Pauly J, Spielman D. Interleaved narrow-band PRESS sequence with adiabatic spatial-spectral refocusing pulses for ^{1}H MRSI at 7T. Magn Reson Med. 2008; 59(5):973–979. [PubMed: 18429014]
4. Hetherington HP, Avdievich NI, Kuznetsov AM, Pan JW. RF Shimming for Spectroscopic Localization in the Human Brain at 7 T. Magn Reson Med. 2010; 63(1):9–19. [PubMed: 19918903]
5. Schuster C, Dreher W, Geppert C, Leibfritz D. Fast 3D ^{1}H spectroscopic imaging at 3 tesla using spectroscopic missing-pulse SSFP with 3D spatial preselection. Magn Reson Med. 2007; 57(1):82–89. [PubMed: 17191249]
6. Schuster C, Dreher W, Stadler J, Bernarding J, Leibfritz D. Fast Three-Dimensional ^{1}H MR Spectroscopic Imaging at 7 Tesla Using “Spectroscopic Missing Pulse - SSFP”. Magn Reson Med. 2008; 60(5):1243–1249. [PubMed: 18836998]
7. Scheenen TWJ, Heerschap A, Klomp DWJ. Towards ^{1}H-MRSI of the human brain at 7T with slice-selective adiabatic refocusing pulses. Magn Reson Mater Phys. 2008; 21:95–101.
8. Tkac I, Oz G, Adriany G, Ugurbil K, Gruetter R. In Vivo ^{1}H NMR Spectroscopy of the Human Brain at High Magnetic Fields: Metabolite Quantification at 4T vs. 7T. Magn Reson Med. 2009; 62(4):868–879. [PubMed: 19591201]
9. Mekle R, Mlynarik V, Gambarota G, Hergt M, Krueger G, Gruetter R. MR Spectroscopy of the Human Brain With Enhanced Singla Intensity at Ultrashort Echo Times on a Clinical Platform at 3T and 7T. Magn Reson Med. 2009; 61(6):1279–1285. [PubMed: 19319893]
10. Tkac I, Andersen P, Adriany G, Merkle H, Ugurbil K, Gruetter R. In vivo ^{1}H NMR spectroscopy of the human brain at 7 T. Magn Reson Med. 2001; 46(3):451–456. [PubMed: 11550235]
11. Mangia S, Tkac I, Gruetter R, Van de Moortele PF, Giove F, Maraviglia B, Ugurbil K. Sensitivity of single-voxel ^{1}H-MRS in investigating the metabolism of the activated human visual cortex at 7 T. Magn Reson Imaging. 2006; 24(4):343–348. [PubMed: 16677939]

12. Terpstra M, Ugurbil K, Tkac I. Noninvasive quantification of human brain ascorbate concentration using ^{1}H NMR spectroscopy at 7 T. NMR Biomed. 2010; 23(3):227–232. [PubMed: 19655342]
13. Garwood M, DelaBarre L. The return of the frequency sweep: designing adiabatic pulses for contemporary NMR. J Magn Reson. 2001; 153(2):155–177. [PubMed: 11740891]
14. Pan JW, Venkatraman T, Vives K, Spencer DD. Quantitative glutamate spectroscopic imaging of the human hippoicampus. NMR Biomed. 2006; 19(2):209–216. [PubMed: 16479532]
15. Scheenen TWJ, Klomp DWJ, Wijnen JP, Heerschap A. Short echo time ^{1}H-MRSI of the human brain at 3T with minimal chemical shift displacement errors using adiabatic refocusing pulses. Magn Reson Med. 2008; 59(1):1–6. [PubMed: 17969076]
16. Michaeli S, Garwood M, Zhu XH, DelaBarre L, Andersen P, Adriany G, Merkle H, Ugurbil K, Chen W. Proton T_2 relaxation study of water, N-acetylaspartate, and creatine in human brain using Hahn and Carr-Purcell spin echoes at 4T and 7T. Magn Reson Med. 2002; 47(4):629–633. [PubMed: 11948722]
17. Xin L, Gambarota G, Mlynarik V, Gruetter R. Proton T_2 relaxation time of *J*-coupled cerebral metabolites in rat brain at 9. 4T. NMR Biomed. 2008; 21(4):396–401. [PubMed: 17907262]
18. Adriany G, De Moortele PFV, Ritter J, Moeller S, Auerbach EJ, Akgun C, Snyder CJ, Vaughan T, Ugurbill K. A geometrically adjustable 16-channel transmit/receive transmission line array for improved RF efficiency and parallel imaging performance at 7 Tesla. Magn Reson Med. 2008; 59(3):590–597. [PubMed: 18219635]
19. Yousry TA, Schmid UD, Alkadhi H, Schmidt D, Peraud A, Buettner A, Winkler P. Localization of the motor hand area to a knob on the precentral gyrus - A new landmark. Brain. 1997; 120:141–157. [PubMed: 9055804]
20. Metzger GJ, Snyder C, Akgun C, Vaughan T, Ugurbil K, Van de Moortele PF. Local B_1^+ shimming for prostate imaging with transceiver arrays at 7T based on subject-dependent transmit phase measurements. Magn Reson Med. 2008; 59(2):396–409. [PubMed: 18228604]
21. Baum J, Tycko R, Pines A. Broadband and adiabatic inversion of a two-level system by phase-modulated pulses. Phys Rev A. 1985; 32(6):3435–3447. [PubMed: 9896511]
22. Silver MS, Joseph RI, Hoult DI. Highly selective $\pi/2$ and π pulse generation. J Magn Reson. 1984; 59(3):347–351.
23. Gruetter R. Automatic, localized *in vivo* adjustment of all first- and second-order shim coils. Magn Reson Med. 1993; 29(6):804–811. [PubMed: 8350724]
24. Gruetter R, Tkac I. Field mapping without reference scan using asymmetric echo-planar techniques. Magn Reson Med. 2000; 43(2):319–323. [PubMed: 10680699]
25. Tkac I, Starcuk Z, Choi IY, Gruetter R. *In vivo* ^{1}H NMR spectroscopy of rat brain at 1 ms echo time. Magn Reson Med. 1999; 41(4):649–656. [PubMed: 10332839]
26. Pfeuffer J, Tkac I, Provencher SW, Gruetter R. Toward an *in vivo* neurochemical profile: quantification of 18 metabolites in short-echo-time ^{1}H NMR spectra of the rat brain. J Magn Reson. 1999; 141(1):104–120. [PubMed: 10527748]
27. Provencher SW. Estimation of metabolite concentrations from localized *in vivo* proton NMR spectra. Magn Reson Med. 1993; 30(6):672–679. [PubMed: 8139448]
28. Provencher SW. Automatic quantitation of localized *in vivo* ^{1}H spectra with LCModel. NMR Biomed. 2001; 14(4):260–264. [PubMed: 11410943]
29. Henry PG, Marjanska M, Walls JD, Valette J, Gruetter R, Ugurbil K. Proton-observed carbon-edited NMR spectroscopy in strongly coupled second-order spin systems. Magn Reson Med. 2006; 55(2):250–257. [PubMed: 16402370]
30. Govindaraju V, Young K, Maudsley AA. Proton NMR chemical shifts and coupling constants for brain metabolites. NMR Biomed. 2000; 13(3):129–153. [PubMed: 10861994]
31. Kaiser LG, Marjanska M, Matson GB, Iltis I, Bush SD, Soher BJ, Mueller S, Young K. ^{1}H MRS detection of glycine residue of reduced glutathione in vivo. J Magn Reson. 2010; 202(2):259–266. [PubMed: 20005139]
32. Pijnappel WWF, Vandenboogaart A, Debeer R, Vanormondt D. Svd-Based Quantification of Magnetic-Resonance Signals. J Magn Reson. 1992; 97(1):122–134.

33. Gasparovic C, Song T, Devier D, Bockholt HJ, Caprihan A, Mullins PG, Posse S, Jung RE, Morrison LA. Use of tissue water as a concentration reference for proton spectroscopic imaging. Magn Reson Med. 2006; 55(6):1219–1226. [PubMed: 16688703]
34. Ernst T, Kreis R, Ross BD. Absolute Quantitation of Water and Metabolites in the Human Brain. 1. Compartments and Water. J Magn Reson B. 1993; 102(1):1–8.
35. Rooney WD, Johnson G, Li X, Cohen ER, Kim SG, Ugurbil K, Springer CS. Magnetic field and tissue dependencies of human brain longitudinal $^{1}H_2O$ relaxation in vivo. Magn Reson Med. 2007; 57(2):308–318. [PubMed: 17260370]
36. Bartha R, Michaeli S, Merkle H, Adriany G, Andersen P, Chen W, Ugurbil K, Garwood M. In vivo $^{1}H_2O$ T_2(dagger) measurement in the human occipital lobe at 4T and 7T by Carr-Purcell MRI: Detection of microscopic susceptibility contrast. Magn Reson Med. 2002; 47(4):742–750. [PubMed: 11948736]
37. Kreis R, Slotboom J, Hofmann L, Boesch C. Integrated data acquisition and processing to determine metabolite contents, relaxation times, and macromolecule baseline in single examinations of individual subjects. Magn Reson Med. 2005; 54(4):761–768. [PubMed: 16161114]
38. Soher BJ, Pattany PM, Matson GB, Maudsley AA. Observation of coupled ^{1}H metabolite resonances at long TE. Magn Reson Med. 2005; 53(6):1283–1287. [PubMed: 15906305]
39. Traber F, Block W, Lamerichs R, Gieseke J, Schild HH. ^{1}H metabolite relaxation times at 3. 0 tesla: Measurements of T1 and T2 values in normal brain and determination of regional differences in transverse relaxation. J Magn Reson Imaging. 2004; 19(5):537–545. [PubMed: 15112302]
40. Michaelis T, Merboldt KD, Bruhn H, Hanicke W, Frahm J. Absolute Concentrations of Metabolites in the Adult Human Brain in Vivo - Quantification of Localized Proton MR Spectra. Radiology. 1993; 187(1):219–227. [PubMed: 8451417]
41. Pouwels PJW, Frahm J. Regional metabolite concentrations in human brain as determined by quantitative localized proton MRS. Magn Reson Med. 1998; 39(1):53–60. [PubMed: 9438437]
42. Tunc-Skarka N, Weber-Fahr W, Hoerst M, Meyer-Lindenberg A, Zink M, Ende G. MR spectroscopic evaluation of N-acetylaspartate's T2 relaxation time and concentration corroborates white matter abnormalities in schizophrenia. Neuroimage. 2009; 48(3):525–531. [PubMed: 19573608]

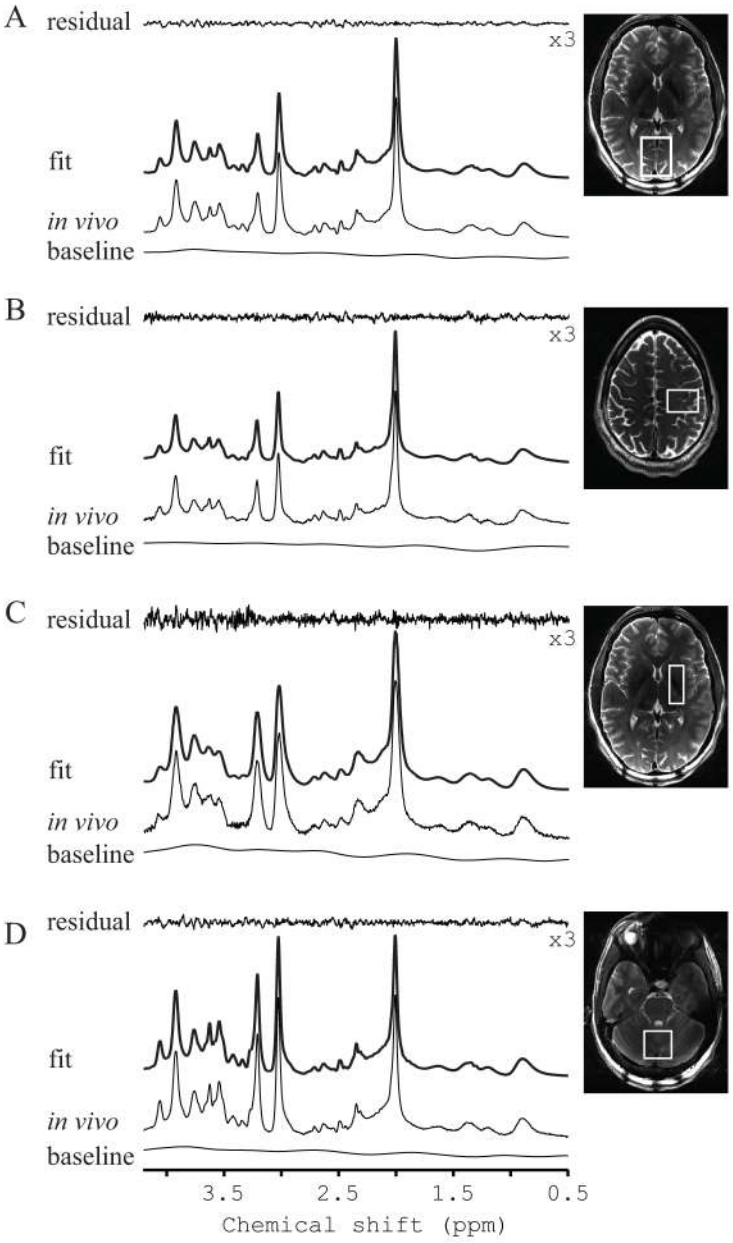

Figure 1.

LCModel quantification of the representative ^{1}H NMR spectra obtained at 7 T with a modified LASER sequence from the four following regions of the human brain: (a) a 19.7 mL voxel placed in the occipital lobe (OC), (b) an 8 mL voxel placed in the motor cortex (MC), (c) a 9 mL voxel placed in the basal ganglia (BG), and (d) a 15.6 mL voxel placed in the cerebellum. In all spectra, T_R = 4.5 s, T_E = 35 ms, N_S = 128, and no line-broadening was applied. The location and size of the voxels are shown on T_2-weighted images.

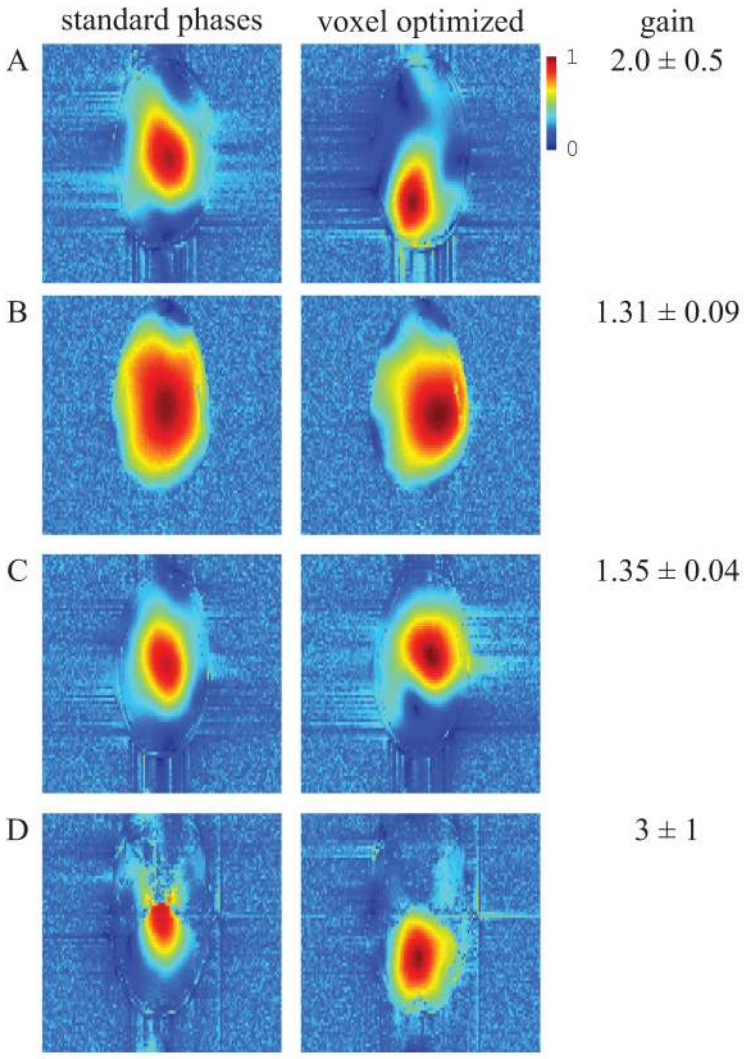

Figure 2.
The relative transmit efficiency before and after local B_1^+ phase shimming, optimized for the following regions of interest: (a) OC, (b) MC, (c) BG, and (d) CR. The average gain and standard deviation ($n = 5$) in the transmit efficiency is listed next to each image.

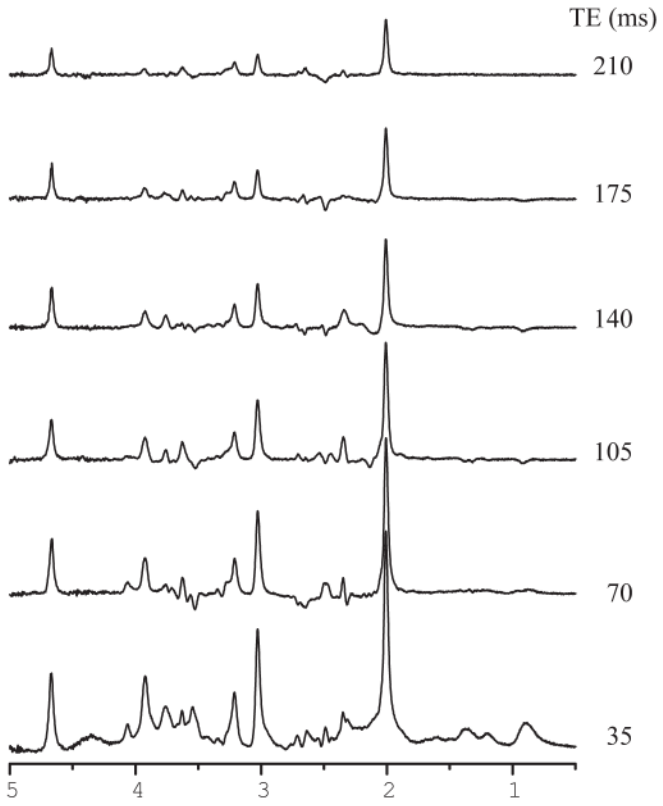

Figure 3.
Representative ^{1}H NMR spectra obtained at 7 T with a modified LASER sequence from the 19.7 mL voxel placed in the human occipital lobe. For the spectra, T_R = 4.5 s, N_S = 64, and no line-broadening was applied.

Table 1

T_2 values (mean ± SD) of water and metabolites measured at 7 T from three subjects per voxel (10 subjects in total). For each substance (water or metabolites) means with different letters in the superscript differ at 0.05 significance level. For all singlet resonances, fits with R^2 ≥0.97 were obtained except for *s*Ins in BG, where $R^2 = 0.85$. For all multiplet resonances, fits with R^2 ≥0.8 were obtained except for mNAA in CR, where $R^2 = 0.54$.

Voxel			**OC**		**MC**		**BG**		**CR**	
	Compound	**Group**	T_2 **(ms)**	R^2	T_2 **(ms)**	R^2	T_2 **(ms)**	R^2	T_2 **(ms)**	R^2
	water		47 ± 1^{b}	0.9991	47 ± 1^{b}	0.9996	41.2 ± 0.8^{a}	0.99993	48 ± 3^{b}	0.9997
singlets	NAA	$^{2}CH_3$	132 ± 6^{a}	0.994	168 ± 6^{b}	0.996	130 ± 11^{a}	0.97	191 ± 7^{c}	0.998
	tCr	$N(CH_3)$	$95 \pm 3^{a, b}$	0.9997	$113 \pm 2^{b, c}$	0.9988	90 ± 11^{a}	0.996	131 ± 8^{c}	0.9991
	tCr	$^{2}CH_2$	84 ± 2^{a}	0.9985	108 ± 5^{b}	0.995	81 ± 15^{a}	0.994	$102 \pm 3^{a, b}$	0.998
	tCho	entire molecule	152 ± 3^{a}	0.992	$139 \pm 9^{a, b}$	0.997	121 ± 5^{b}	0.984	200 ± 17^{c}	0.996
	*s*Ins		96 ± 8^{a}	0.95	112 ± 4^{a}	0.96	80 ± 20^{a}	0.85	130 ± 20^{a}	0.87
J-coupled	NAA	$^{3}CH_2$	90 ± 11^{b}	0.80	110 ± 30^{b}	0.80	69 ± 12^{b}	0.85	170 ± 12^{a}	0.536*
	Glu	entire molecule	93 ± 4^{b}	0.95	98 ± 4^{b}	0.985	88 ± 10^{b}	0.96	139 ± 8^{a}	0.93
	GSH	entire molecule	61 ± 3^{a}	0.88	97 ± 8^{b}	$0.74^{\#}$			$80 \pm 10^{a, b}$	0.908
	*m*Ins	entire molecule	95 ± 2^{b}	0.982	100 ± 15^{b}	0.988	87 ± 6^{b}	0.988	160 ± 20^{a}	0.985
	Tau	entire molecule	$93 \pm 7^{a, b}$	0.80	$90 \pm 16^{a, b}$	0.8	85 ± 10^{b}	0.89	120 ± 20^{a}	0.83

Means with a different letters were significantly different with the significance level of 0.05. Means with the same letter were not significantly different.

All *p* values were below 0.04 for each subject, each metabolite and each region except for (*) mNAA in CR where *p* values were 0.095, 0.099, 0.099, and for ($^{\#}$) GSH in MC where for one subject *p* value was 0.1.

Table 2

SNR values of metabolites measured from spectra in Figure 3.

	SNR					
T_E (ms)	tCr at 3.03 ppm	mNAA	Glu	*m*Ins	GSH	Tau
35	292.9	51.0	82.3	78.5	37.2	23.2
70	210.9	39.8	57.8	72.6	18.9	7.8
105	187.8	30.5	80.3	76.2	17.4	8.4
140	115.9	23.6	49.9	24.5	15.5	7.6
175	97.9	51.1	22.9	39.6	1.9	7.8
210	60.3	17.9	18.0	31.1	4.8	3.8

Table 3

Average brain metabolite concentrations measured with a modified LASER sequence at 7 T (n = 5, 18 subjects, 6 subjects are the same as in Table 3) and quantified using LCModel, SD, and average CRLBs and SD of CRLB.

	OC				MC				BG				CR			
Metabolite	**Conc. (μmol/g)**	**SD (μmol/g)**	**CRLB (%)**	**SD (%)**	**Conc. (μmol/g)**	**SD (μmol/g)**	**CRLB (%)**	**SD (%)**	**Conc. (μmol/g)**	**SD (μmol/g)**	**CRLB (%)**	**SD (%)**	**Conc. (μmol/g)**	**SD (μmol/g)**	**CRLB (%)**	**SD (%)**
Asc	0.4[a]	0.3	26	8	1.2[a]	0.5	19	7	1.5[a]	0.8	18	9	0.6[a]	0.2	28	13
Asp	2.9[a]	0.8	9	2	2.6[a]	0.3	14	2	1.2[b]	0.5	35	9	1.1[b]	0.4	27	14
GABA	1.5[b]	0.3	15	4	0.8[b]	0.6	29	9	1.7[a]	1.3	22	6	1.5[b]	0.5	18	6
Glu	9.6[a]	1.3	1.6	0.5	7.6[b]	0.9	2.4	0.5	6.7[b]	1	3.0	0.7	8.2[a, b]	0.6	2	0
Gln	1.5[b]	0.5	13	6	1.0[b]	0.3	29	7	1.6[b]	0.6	23	11	2.9[a]	0.7	7.2	0.8
Gly	0.7[a]	0.1	9	1	0.5[b]	0.1	20	5	--	--	--	--	0.59[a, b]	0.07	12	2
GSH	1.1[a]	0.1	4.0	0.7	0.7[a]	0.1	7.6	0.5	1.1[a]	0.4	7	3	1.11[a]	0.06	4.4	0.5
mIns	6.4[a, b]	0.8	2	0	5.9[a, b]	0.3	2.6	0.5	5.1[b]	1.4	4.0	0.7	7.4[a]	0.8	2	0
sIns	0.4[a]	0.1	6	2	0.21[a]	0.06	13	4	0.5[a]	0.3	10	4	0.4[a]	0.2	7	3
NAA	12.6[a]	1.7	1	0	10.5[a, b]	1.2	1	0	7.8[c]	0.4	1.8	0.4	8.4[b, c]	1	1	0
NAAG	0.40[a]	0.2	18	6	1.6[b]	0.4	7	3	0.8[a, b]	1.1	21	18	1.0 [a, b]	0.2	6.0	0.7
PE	2.3[a]	0.4	7	1	1.1[b]	0.4	23	7	1.3[b]	0.5	19	3	1.3[b]	0.4	15	5
tCho	0.9[c]	0.1	2	0	1.32[b, c]	0.09	2.2	0.4	1.5[b]	0.4	3.2	0.4	2.2[a]	0.2	1	0
tCr	8.7[a, b]	1.1	1	0	7.4[b]	0.6	1.2	0.4	8[b]	2	2	0	10.2[a]	0.9	1	0
Lac + Thr	0.8[a]	0.2	10	4	0.9[a]	0.3	11	3	0.6[a]	0.1	20	10	1.0[a]	0.5	9	2
Glc + Tau	2.1[b]	0.3	7	2	1.7[b]	0.2	8	4	1.8[b]	0.6	9	1	3.5 [a]	0.4	4	1

Fractional tissue composition	**OC**	**MC**	**BG**	**CR**
CSF	0.05 ± 0.02	0.08 ± 0.02	0.001 ± 0.0009	0.07 ± 0.05
GM	0.51 ± 0.05	0.19 ± 0.03	0.25 ± 0.06	0.72 ± 0.14
WM	0.44 ± 0.05	0.73 ± 0.02	0.73 ± 0.05	0.19 ± 0.16

Means with a different letter were significantly different with the significance level of 0.05. Means with the same letter were not significantly different.

The concentrations of following metabolites were based on assumed T_2 values: Asc, Asp, GABA, Gln, Gly, NAAG, PE, Lac + Thr, Glc + Tau.